Multi-configuration model tuning for precision opto-mechanical systems

Deborah J. Howell[a], Olivier de Weck, Ph.D.[b] and Carl Blaurock, Ph.D.[c]

[a]Massachusetts Institute of Technology, 77 Mass. Ave., 37-346, Cambridge, MA, USA
[b]Massachusetts Institute of Technology, 77 Mass. Ave. 33-410, Cambridge, MA, USA
[c] Mide Technology Corp., 3916 Lauriston Rd., Raleigh NC 27616

ABSTRACT

High quality multi-disciplinary integrated models are needed for complex opto-mechanical spacecraft such as SIM and TPF in order to predict the system's on-orbit behavior. One major activity in early design is to examine the system's behavior over multiple configurations using an integrated model. A three step procedure for model tuning is outlined that consists of (1) applying engineering insight to the model so that all physical systems are present in the model, (2) using optimization to automatically update system parameters that are uncertain in the model, and (3) evaluating the model at several configurations using the updated parameters. The key contribution of this work is the systematic checking of the validity of the updated parameters by evaluating, both in the model and the experiment, the system at different configurations (step three). It is hypothesized that if the simulation model and experimental data of the additional configurations match well then the tuned system parameters were indeed updated in a way that physically represents the system. This three step process is applied to a testbed at the MIT Space System Laboratory.

Keywords: integrated modeling, model updating, configuration

1. INTRODUCTION

The next generation of space telescopes being developed by NASA are extremely complex multidisciplinary systems that often require models with predictive capability in the nanometer range (e.g. James Webb Space Telescope, Terrestrial Planet Finder, Space Interferometry Mission). In the planning and design phases, developers routinely rely on simulation models to determine hardware configuration and to estimate and improve performance and cost. This paper focuses on the development of physically accurate open loop simulation models that are valid for configuration changes either in the pre-hardware stage, or after a prototype hardware model has been built. A physically accurate simulation model will enable modelers to evaluate the system over a larger tradespace and to perform optimization, uncertainty, and sensitivity analyses. Configuration changes imply component redistribution (changes of form) rather than changes in functionality. These types of changes include, but are not limited to, mass, material, and geometric changes. Integrated models that are accurate across configuration changes have immense value. The developer is able to change the simulation model relatively easily and immediately see performance and cost changes, which in turn reduces performance risk. In this way meaningful optimization and sensitivity studies can be performed. Several papers and theses have been written on the process and application of integrated modeling of space structures (Melody,[1] Gutierrez,[2] de Weck,[3] Shaklan[4]). In integrated modeling, multiple aspects of the system (i.e. structures, controls, optics) are combined into a single linear model, generally using the state space representation. The scope of this paper and its application are limited to this linear modeling process.

The procedure presented here for open-loop finite element model updating is laid out in three steps. Step 1, Coarse Tuning/Model Topology, makes use of engineering insight to take out non-parametric (and some parametric) error from the model, such that all the important components and interfaces are properly represented in the model. The next step, Automated Tuning, employs classical model tuning. The third and final step, Model Validation and Tracking, verifies that the simulation model produced in Step 2 tracks across configuration changes. Iterations between Steps 1, 2, and 3 might be necessary (see Figure 1). The hypothesis of this paper

djhowell@mit.edu Tel: 1 617 253 8364

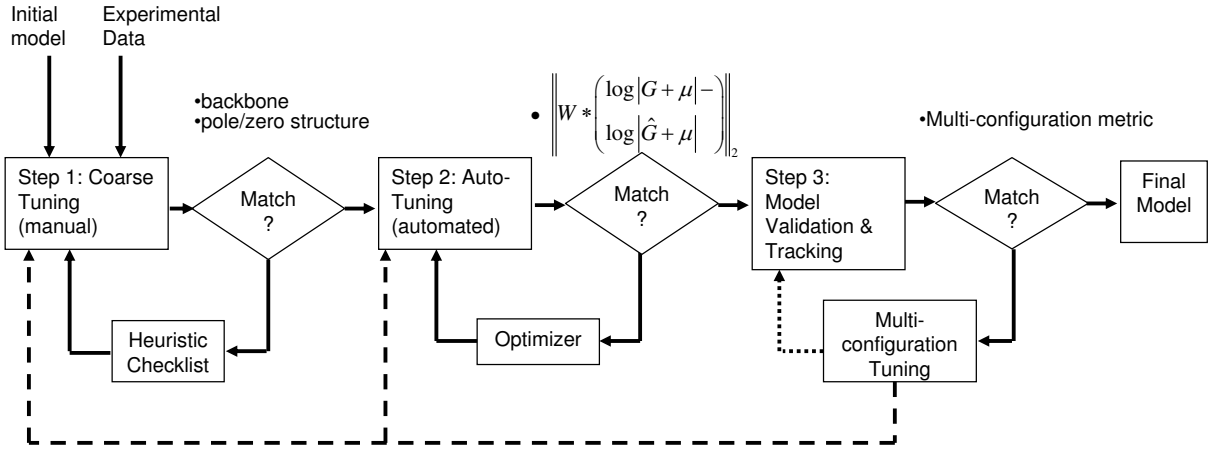

Figure 1. Three Step Procedure Flow Diagram

can be stated as: **The three step tuning procedure is more robust in terms of physical model tuning across configurations than single point (manual or automatic) model tuning.** Models are often tuned to minimize model-experiment mismatch, however there are typically many more parameters in the model than mismatch metrics that can be measured - this is a problem of non-uniqueness. Therefore models are very often tuned in a non-physical way. The three step procedure strives to tune the model in a physical way by examining more than one configuration. This can be stated as $\min_{\mathbf{p}} \sum_i (\mathrm{J_{exp}} - \mathrm{J_{model}})_i$ subject to $\mathbf{p}_{LB} \leqslant \mathbf{p} \leqslant \mathbf{p}_{UB}$, where $(\mathrm{J_{exp}} - \mathrm{J_{model}})_i$ represents the mismatch metric for the i^{th} configuration, $\mathbf{p}$ is the vector of parameters, $\mathbf{p}_{LB}$ is the lower parameter bound, and $\mathbf{p}_{UB}$ is the upper parameter bound.

The three step process will be applied using a complex structural test article built at the Space Systems Laboratory at MIT called OPTSIM. The process can be applied to multidisciplinary systems, but here a purely structural system is addressed. Note that references to previous work are distributed throughout this paper.

2. STEP 1: COARSE TUNING

Table 1 enumerates heuristic rules that the modeler can invoke to ensure that the non-parametric error is significantly reduced so that the basic/important dynamics are captured in the model. They are a compilation of engineering insights usually performed by an engineer using his experience and intuition. Checks that are easy to perform, yet provide a relatively large amount of error reduction are at the beginning of this list. Checks that are difficult to carry out and only reduce the error by a relatively small amount are towards the end of the list. This ordering is based on the authors experience and can change given a different system. It is only a guide and it is up to the modeler to choose the appropriate order. These heuristics are based on engineering insight from Glaese,[5] Campbell,[6] and Stockwell.[7] Even though these heuristics are listed in order to reduce non-parametric error, they also, to an extent, help to reduce parametric error. A section on overall implementation of these heuristics is provided in Howell.[8] Once these checks are complete, the modeler should have a model with little or no non-parametric error, or at least a model that is a better representation the system. It should be noted that the mismatch metric does not necessarily improve as one steps through the heuristics of Table 1. The structure of the system (e.g. the pole/zero sequence in the transfer function) should, however, improve by the end of Step 1.

2.1. Metrics for Model Matching

The extent of model/experiment matching will primarily be evaluated using frequency response or transfer functions because they are easy to obtain and provide valuable insight into the system's dynamics. Some alternatives include time domain output responses. The transfer function was chosen here because it incorporates

Table 1. Summary of Model Heuristics

Model Heuristic	Description
Typographical Errors	Reality check for all parameter values and consistent units of measurement
Mass and Inertia	Total and component weights & inertias
Component properties	Stiffness, inertial, geometric and placement properties (only once assembled in subsystem)
Finite element code	Sound implementation of FE program
Element types	Element assumptions should reflect physical reality
Boundary conditions	Fixed, pinned, free conditions at model boundaries
Sensors and actuators	Position, orientation, and calibration
Gravity effects	Presence of gravity or off-loading conditions
Discretization	Fineness of finite element meshing or number of states
Linearity	Identify linear and non-linear system regimes
Modal Survey	Match simulated modes with measured modes
Damping	Modal, complex, mode-by-mode damping
Interfaces	Boundary conditions and compliance at important interfaces, impedance matching

the input and output dynamics in the frequency domain; this provides an easy way to analyze a large amount of data. Also, noise can be averaged out of the system easily when working in the frequency domain. Two good references on the process of obtaining frequency domain data are Ewins[9] and Maia.[10] An integrated model is generally represented in state space, and the transfer function is easily obtained from the state space representation using[11] $\mathbf{G}(\omega) = \mathbf{C}(j\omega\mathbf{I} - \mathbf{A})^{-1}\mathbf{B} + \mathbf{D}$. In the above equation, $\mathbf{G}$ represents the complex transfer function and $\mathbf{A}$, $\mathbf{B}$, $\mathbf{C}$ and $\mathbf{D}$ are the state space matrices. Before moving on to automated model tuning, there should be some degree of matching between the data and the analytical model. First of all, the low and high frequency asymptotes of the transfer function(s) should align. This check can be performed on visual inspection. Secondly the slope of the transfer function backbone should match. This is called the dereverberated transfer function backbone, and it is the transfer function of the local effects (underlying trend) while ignoring the reverberant (far-field) effects. The backbone can be calculated using wave theory, by cepstral analysis,[12] or by smoothing the transfer function. Next the sequence of poles and zeros should be compared. This is an easy task for a single-input/single-output (SISO) system, but for a MIMO system, examining the pole/zero sequence involves examining the transfer function of each input/output pair, a very involved job. If the pole/zero sequences line up, then a comparison of the modal frequencies can take place. A metric that measures the degree of mismatch for these modal frequencies is $\xi = \left|\frac{\hat{\omega}_i - \omega_i}{\omega_i}\right|$. Here i is the modal number, $\hat{\omega}$ is the analytical modal frequency, and ω is the measured modal frequency. This metric should be small compared to one (below about 0.10 is a good rule of thumb) for every mode in the frequency range of interest.

One could also employ time-domain data or modeshape information to evaluate model/experimental matching. Raw time-domain data, however, is difficult to compare to finite element matrices. Complete modeshape data is near impossible to collect on large systems in the practical sense, especially for rotational degrees of freedom. There are modal expansion techniques that make use of the available and analytical modeshapes in order to produces a complete set of modeshape data (Lipkins and Vanderurzen[13] and Harder[14]). Once the complete modeshape data is assembled (measured or expanded), the experimental and analytical modeshapes can be compared. One method is to check the orthogonality condition, $[\phi]^{\mathrm{T}}[M][\phi] = [I]$, where $[I]$ is the identity matrix and $[\phi]$ is the matrix of mass normalized eigenvectors. The experimental eigenvectors are substituted into the orthogonality condition, and the deviation from the identity matrix is observed. If the diagonal values are near unity for a particular mode, then that mode can be considered correlated to the respective analytical mode. Another method of comparing modeshapes is called the Modal Assurance Criterion (MAC).[15] MAC

values near unity identify highly matched modes. If the values for MAC are poor (near zero), then the error can be physically localized using the Coordinate Modal Assurance Criterion (COMAC). The correlation at each degree of freedom is averaged over each set of correlated mode pairs. Degrees of freedom with a low value of COMAC indicate regions in the system where there is poor experimental/analytical correlation.

3. STEP 2: AUTOMATED TUNING

Much of the research done on the topic of model updating for complex space structures has been in the realm of automated tuning (Gutierrez,[2] Natke,[16] Flanigan,[17] Caesar,[18] Maia[19]), whereby both a simulation model and experimental data are available. In general for complex systems, the experimental results do not match the initial simulation, and model updating is required. Classical model updating consists of changing selected parameter values in order to minimize a measure of mismatch between experimental and simulation results. This is considered to be a mature and established process for model updating. Parametric error can occur when these parameter values are changed improperly. An updated model, however, can contain both parametric and non-parametric error.

Automated tuning is an established process that can be found in the cited literature. An overview is provided here. Parameters can be chosen in a variety of ways, but a popular way is to calculate the normalized sensitivities of the measured performance to each suspect parameter, $\frac{\Delta J/J}{\Delta p/p} \simeq \frac{p_0}{J(p_0)} \cdot \frac{\Delta J}{\Delta p}$, where J is the performance metric of the model/simulation, and p is the parameter. This can be interpreted as a percent change in cost per percent change in the parameter. This finite differencing approach is the most practical way of obtaining sensitivities, since the integrated system might be too complex to obtain analytical results. Finite differencing has two main drawbacks: it is computationally expensive for many parameters and its error depends strongly on parameter step size, Δp. A more rigorous and more favorable approach to sensitivity is to solve for the analytical sensitivity since the cost function can be non-linear. This is sometimes difficult to do for large, complex systems that are most easily modelled using finite elements. The analytical sensitivities of the eigenvalues and eigenvectors with respect to the chosen parameters, are given by Equations 1 and 2, respectively.[19]

$$\frac{\partial (\omega)_i^2}{\partial p_k} = [\phi]_i^{\mathrm{T}} \left[\frac{\partial [\mathbf{K}]}{\partial p_k} - (\omega)_i^2 \frac{\partial [\mathbf{M}]}{\partial p_k} \right] [\phi]_i \tag{1}$$

$$\frac{\partial [\phi]_i}{\partial p_k} = \sum_{j=1, j\neq i}^{N} \frac{[\phi]_j [\phi]_j^{\mathrm{T}}}{(\omega)_i^2 - (\omega)_j^2} \left[\frac{\partial [\mathbf{K}]}{\partial p_k} - (\omega)_i^2 \frac{\partial [\mathbf{M}]}{\partial p_k} \right] [\phi] - \frac{1}{2} [\phi]_i [\phi]_i^{\mathrm{T}} \frac{\partial [\mathbf{M}]}{\partial p_k} [\phi]_i \tag{2}$$

Using Equation 3, $\frac{\partial \omega_i^2}{\partial p_k}$ can be converted to $\frac{\partial \omega_i}{\partial p_k}$.

$$\frac{\partial \omega_i}{\partial p_k} = \frac{1}{2\omega_i} \frac{\partial \omega_i^2}{\partial p_k} \tag{3}$$

These analytical sensitivities can be easily found using the DOCS toolset. * Once the parameters are selected, bounds must be put on those parameters to ensure that the parameters are updated in a physically plausible way. These bounds can be chosen based on prior experience of the modeler, testing of the components, or material studies found in literature.

The optimization problem which chooses the parameter values based on some calculated performance can be stated as $\min_p J(x)$ such that $p_{LB} \leq p \leq p_{UB}$, which minimizes the cost function (J) by varying the chosen parameters (p), subject to lower and upper bounds (p_{LB} and p_{UB} respectively) on those parameters. The x vector contains all the parameters required of the function, J, a subset of which is p. There are several optimization routines from which to choose (least-squares, simulated annealing, genetic algorithms). The selection should be

*DOCS (Disturbance-Optics-Controls-Structures[20]) is a software toolset that is able to assemble separate discipline models into an integrated model which can be explicitly defined as a function of design variables. This enables tradespace exploration and sensitivity analysis in an analytical environment.[21]

made based on the number of parameters, the continuity and linearity of the design space, the computation time associated with the evaluation of the cost function at each iteration, and whether the parameters take on discrete or continuous values. Optimization is a very mature and involved topic; two good references on optimization are Vanderplaats[22] and Papalambros.[23]

Some conventional matching metrics are shown below.

$$\begin{aligned} J_{\text{modal}} &= \sum_{i=1}^{nm} \left[\left(\omega_{\text{model}}(i) - \omega_{\text{experimental}}(i) \right) \right]^2 \\ J_{\text{phase}} &= \left\| \mathbf{W} * \left(\log\left(\mathbf{G} + \mu \right) - \log\left(\hat{\mathbf{G}} + \mu \right) \right) \right\|_2 \\ J_{\text{magnitude}} &= \left\| \mathbf{W} * \left(\log\left| \mathbf{G} + \mu \right| - \log\left| \hat{\mathbf{G}} + \mu \right| \right) \right\|_2 \end{aligned} \tag{4}$$

Here J represents the mismatch metric, its subscript denotes the type of metric. The matrix $\mathbf{W}$ is a weighting matrix, the matrix $\mathbf{G}$ is a transfer function matrix, and μ describes the noise level in the measurement system.

4. STEP 3: MODEL VALIDATION AND TRACKING

4.1. Purpose

A chief purpose of developing a simulation model is to be able to evaluate and optimize the performance and cost associated with configuration changes without the expense of building a new hardware model. However, there must be some degree of confidence that this model is valid across these configurations changes in order for the optimization to have validity. One of the dangers of automated tuning is that if there is more than one parameter to be tuned there is no guarantee that the parameters are tuned in a way that produces a physical model. A model tuned in a non-physical way might match experimental data well for the current configuration, but it is not guaranteed to match for configuration changes, whereas a model tuned properly will track across configurations. It is essential to validate that the parameters were tuned in a physical way in Step 2. This can be verified by perturbing the testbed and the simulation model together to see if they track along configuration changes. If the model does track, then there is greater confidence that the model physically represents the system and is appropriate for optimization.

4.2. Method

A configuration change is implemented in the hardware model, and a corresponding change is made in the updated simulation model. One or several new configuration systems can be constructed this way. Next, the multi-configuration metric, described in the next section, is applied to determine how well the simulation model tracks across configurations.

4.3. Multi-Configuration Metrics

A unique way of assessing the validity of the model (and also by allowing the new costs to exceed the original costs by a small amount) is to first construct the following matrix, $\mathbf{Y}$, which is symmetric positive definite.

$$\underset{\mathrm{k+1}\times\mathrm{k+1}}{\mathbf{Y}} = \frac{1}{\mathrm{J_t^2}} \begin{bmatrix} \mathrm{J_t^2} & \mathrm{J_tJ_1} & \mathrm{J_tJ_2} & \cdots & \mathrm{J_tJ_k} \\ & \mathrm{J_1^2} & \mathrm{J_1J_2} & \cdots & \mathrm{J_1J_k} \\ & & \mathrm{J_2^2} & \cdots & \mathrm{J_2J_k} \\ & \text{Sym.} & & \ddots & \vdots \\ & & & & \mathrm{J_k^2} \end{bmatrix} \tag{5}$$

The variable $\mathrm{J_t}$ represents the mismatch of the original model and $\mathrm{J_1}, \mathrm{J_2} \ldots \mathrm{J_k}$ represent the mismatch of the subsequent configurations. The infinity norm of $\mathbf{Y}$ (maximum absolute row sum) is then evaluated and divided by the number of configurations (original plus new). This value, called the multi-configuration metric, contains information about the distribution of the costs as well as the distance between the new configuration costs and the original cost. It is then compared against a threshold number, T (see Equation 6). If it exceeds the threshold

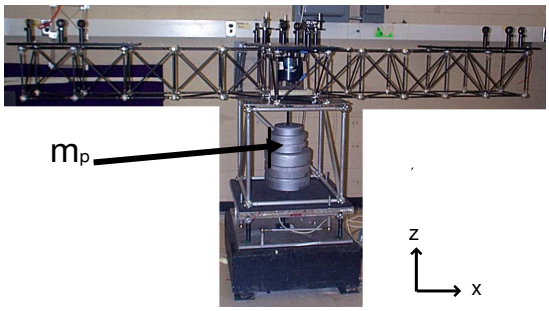

Figure 2. OPTSIM: General View

number, then the model is rejected; if the multi-configuration metric is below the threshold number, the model is accepted.

$$\frac{\|\mathbf{Y}\|_\infty}{(\mathrm{k}+1)} \leq \mathrm{T} \tag{6}$$

The threshold number is defined by the modeler and can be greater than or equal to 1.0. A threshold number of 1.0 approximately corresponds to a scenario where none of the new configurations performance values exceed the original performance value, with a small allowable distribution around the original cost. Increasing the threshold number increases the range in which new configuration costs are allowed to exceed the original cost. It is not recommended that the threshold number exceed 2.0 since this would indicate configuration costs that far exceed the original cost. In Howell[8] the three step procedure is thoroughly illustrated on a simple beam-spring system.

5. EXPERIMENTAL APPLICATION

The testbed OPTSIM (Optical Performance Testbed for Space Interferometry Models) was developed in order to illustrate the three step procedure. This system is complex enough to illustrate the problems encountered on space flight systems, yet it is simple enough to model and to understand the basic dynamics. OPTSIM was built at the Space Systems Laboratory at MIT and was designed to structurally represent a spacecraft interferometer. The central structure (bus area, disturbance source, and one truss bay) was built for experimental validation in de Weck.[24] The upper truss boom (11 bays) and optical mounting plates were subsequently added in order to include optics and controls capability. The entire testbed is supported at each of the four corners by identical vertically mounted springs which sit on a large rectangular cement block . This structure has the potential for a multi-disciplinary analysis, but only the structural model will be address in this work. The input to the system is a disturbance force provided by a shaker (Brüel & Kjaer Vibration Exciter Type 4809) which is located inside the small central bay above the bus. It can provide up to 44.5 N of force in the vertical direction, with a frequency range of 10 Hz to 20 kHz. In addition, there is a load cell attached to the shaker that records the force input to the system (Model 208A02). The force provided by the shaker can be changed by varying the input voltage (Vs). The output of the system is the vertical (z-direction) displacement of the composite base plate as measured by an eddy current gap sensor (Bentley XL 5mm). All subsequent transfer functions shown in this paper will relate the gap sensor output to the load cell input with the units $\frac{\mu m}{N}$.

The final tuned model will be compared with a model that is manually tuned to a single configuration using trial and error parameter changing, a traditional way of tuning a model (see Section 5.5). By performing experimental validation, the hypothesis that the proposed three step procedure is useful in discerning a physically appropriate simulation model will be supported.

5.1. Initial Simulation Model

Since this system is purely structural (no controls or optical metrics), it can be completely modelled using the finite element method (FEM). This is assumed to be a steady state problem, with no controlled actuators, and therefore no sensor and actuator dynamics. The initial simulation model was defined using MSC/NASTRAN

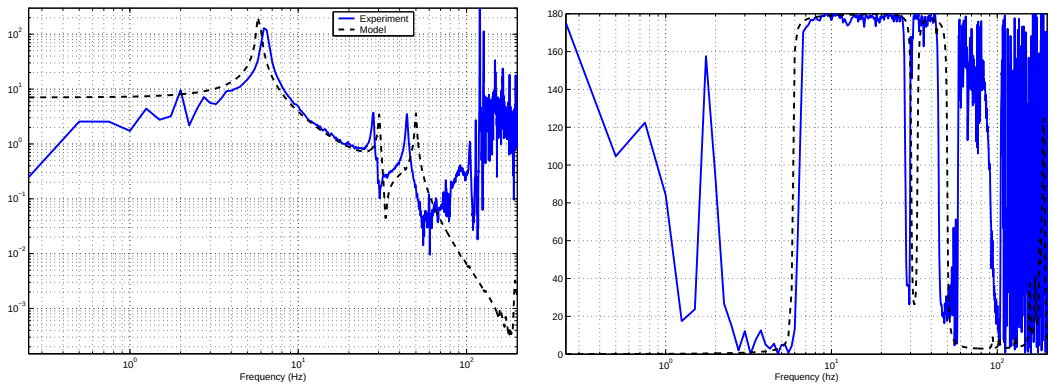

Figure 3. (a) Initial Model and Experimental Transfer Function $\frac{\mu m}{N}$ for Bus Mass = 100 lbs, Model Input Voltage = 0.3Vrms(b) Initial Model and Experimental Phase (deg)

2001. The overall structure is made up of beam, plate, spring, and concentrated mass elements. The modal damping was initially set to 0.01 for all modes. A SISO state space model is built, and the corresponding transfer function (shaker force input to gap sensor output) can be extracted. The model transfer function can then be compared directly with the experimentally determined transfer function, which can be seen in Figure 3. Several things can be observed from Figure 3. Within the valid region (5-100 Hz as determined by the experimental coherence function, not shown here), the transfer functions seem to match well. First, the roll-off (slope of the transfer function) from the first mode to about 60 Hz matches well at approximately -40 dB/dec. Secondly, the low frequency asymptote (at 4 Hz) matches well. It is not immediately clear that the high frequency asymptote matches, since there is a definite roll-up of the experimental transfer function after about 60 Hz. However, at 100Hz, unidentified modes might be obscuring the asymptote line. The pole/zero sequence within the valid region seem to match as well (pole-pole-zero-pole). While the first model mode (at about 6 Hz) under-predicts the experimental frequency, the second and third model modes (30 Hz and 50 Hz) are both high with respect to the frequency of the experimental modes.

5.2. Step 1: Coarse Tuning

This experimental data described in the previous section will now serve as the "truth" model. All subsequent changes will be made to the simulation model in order to reproduce the experimental data. Now we will step through the checklist provided in Table 1. First, the linearity is checked by changing the magnitude of the force input into the system - the resulting transfer functions should not change appreciably, and they do not within the valid range. Even though linearity is towards the end of the list in Table 1, it is performed first since a linear model is being used and because the check is easy to perform experimentally. Next, we can focus on aligning the transfer functions in Figure 3. The fundamental mode contributes the most to the output displacement (highest magnitude mode in the transfer function), therefore it will be addressed first. Its corresponding modeshape shows the testbed (from the baseplate up) moving up and down on the supporting springs. Therefore, its frequency depends heavily on the properties of the spring and the total mass of the testbed. The value for the spring constant in the model was taken directly from the product specifications (168 lbs/in). The average experimental value, however, was determined to be 145.25 lbs/in in the region of interest (m_p = 0 to 200 lbs) *. The fundamental mode decreases in frequency with the smaller spring constant, as expected (from 5.75 Hz to 5.5 Hz). Also, the frequencies of the second and third modes remain unchanged. Since the frequency of the fundamental mode depends so heavily on the spring constant and total mass of the system, this transfer function implies that there might be extra mass present in the simulation model. The mass of the components was measured to best of the author's ability, and the total mass of the testbed was experimentally determined to be

*Testing performed in part by Olivier de Weck[24]

Table 2. Modal Frequency (Hz)

Mode No.	First	Second	Third
Experimental Modes	6.25	28.0	44.25
Initial Model	5.84	30.30	50.00
Changed Spring Constant	5.55	30.26	50.00
Changed Breadboard Mass	5.53	30.03	49.75
Added Gravity Field	5.53	30.03	49.75
K6ROT	5.48	30.02	49.73
Moved Sensor	5.48	30.02	49.73

Table 3. Percent Frequency Errors

Mode No.	Experimental Modes	Model Modes	$\frac{F_{mod}-f_{exp}}{f_{exp}}$
First	6.25	5.48	0.1232
Second	28.00	30.02	0.0721
Third	44.25	49.73	0.1238

105.9 kg. The weight of the modelled system is 102.7 kg, a difference of only 3%. Upon careful consideration of the possible sources of this error, the optical breadboards and components were re-measured. They were determined to be slightly heavier than the model was predicting. This was changed in the model, and the total model mass increased to 103.3 kg, lowering the error to 2.5%. A possible source of error here is the compounding effect of small errors in the mass of the truss bars or truss nodes. There are 184 truss bars and 64 nodes, so a small error in the mass of one truss bar (5 g), produces a large overall error (0.92 kg). Another possible source of error is the measurement error.

Next, a gravity field was added to this model, but it produces no appreciable difference (see Table 2). The initial condition for the finite element dynamic analysis, however changed. This condition consisted of the the compression of the base springs and a drooping of the truss arms.

A known problem in finite element software has to do with the rotation of the plate elements about their normal axis. In the initial model all the plate z rotations were constrained using single point constraints. However, NASTRAN provides a parameter (K6ROT) that resists motion in that degree of freedom, and eliminates the singularities that form in the K matrix (due to excessive pivot ratios). By removing the single point constraints, and introducing this new parameter, the boundary conditions were amended, and the singularities were avoided. Table 2 shows the new modal frequencies using the K6ROT parameter.

The location of the gap sensor was originally modelled to be in the direct center of the base plate. Upon re-measuring, this position was found to be slightly incorrect. The sensor placement on the model was then moved the appropriate amount. This position change does not affect the system's modal frequencies but the change should be visible in the transfer function.

Table 3 shows the results of the altered model incorporating all of the changes described in this section. The experimental and model transfer functions not only have the same pole/zero sequence and the same roll-off, but also are very similar in terms of modal frequency. Table 3 shows that the frequency error is below ten percent for the second mode, but is about 12% for the first and third modes. Furthermore, the objective function cost, as given by the second equation in 4 (log-cost) can also be computed for the initial and fitted models. The cost for the initial model is 3.7662 and the cost for the new model is 4.4368, which indicates a slight worsening in the model-experiment matching. Even though the model has been worsened in terms of the objective function cost, it has been improved since non-parametric error has been reduced. Since all of the non-parametric errors identified in this section were implemented in the model properly, this model will be retained. This will be considered sufficient for the present problem and proceed to the next step: Automated Model Updating.

Table 4. Updated Parameter Values

Parameters	Original Value	Updated Value	Percent Change
Spring Constant	29198.27	3.0658e+4	5.0
Young's Modulus (Plate)	7.20+10	6.4800e+10	-10.0
Young's Modulus (Links)	7.20+10	7.7767e+10	8.0
Damping ratio 1^{st}	0.01	0.0876	876.0
Damping ratio 2^{nd}	0.01	0.0487	487.0
Damping ratio 3^{rd}	0.01	0.0672	672.0

5.3. Step 2: Automated Model Updating

An analytical sensitivity analysis was performed on this system with respect to its structural elements. The sensitivity result is measured in units of root mean square output performance (in this case, displacement of the base plate in μm as measured by the gap sensor). These sensitivity values show the relative impact of a similar percentage change of each parameter on the base plate displacement. The sensitivity analysis indicates that the most sensitive components are the Young's modulus of the top aluminum plate and the rotational links, and the spring constants. These are the parameters that will be chosen for the automated updating. The Young's modulus parameters are both for aluminum. The various aluminum alloys found in[25] have a variation of about +/- 7%. These values (plus a buffer amount of 3%) are used as a guide for the upper and lower bounds. The spring constant was experimentally determined earlier, but this could be incorrect due to measurement error. If it is assumed that the distance measurement was accurate only to 0.1 inches, and that the weight measurement was accurate only to 1 lbs., then the corresponding variation in the spring constant would be +/-2.0%. A buffer of 3% is also added. The modal damping coefficients are also added as parameters to be updated.

The chosen cost function is the logarithmic frequency response error, Equation 4. The frequency response will be weighted in the cost function according to the valid range. From 5 - 100 Hz, the weighting will be 1.0, and outside that range, the weighting will be 0.1; this effectively discounts the regions where the coherence is low. Transfer function values below 0.07 will be ignored by this algorithm; this simulates the noise floor. The automated updating was performed using DOCS updating code.[20] The updated parameter values can be seen in Table 4. Substantial improvement occurs in the model/experimental mismatch metric, however, there is still an appreciable error in each mode. Note that from Table 4 the spring constant and Young's modulus of the plate are both at their extremes (+5% and -10.0%, respectively), this would indicate that increasing the spring constant and/or decreasing the plates Young's modulus further would cause the model to match better to the experiment. However, these further changes would not produce a physically meaningful model. The mismatch metric values for the initial model, the model after Step 1, and the model after Step 2 (tuned model) are 3.7662, 4.4368, and 1.3942 respectively. The objective function cost has decreased by more than 60% due to the changes made using automated tuning.

5.4. Step 3: Model Validation and Tracking

The next step is to change the configuration of the system, and to observe the change in the updated simulation model and in the testbed response. These altered systems will then be compared to determine if the correct parameters where changed in the proper way in Step 2. The change implemented was to alter the mass of the bus in the center of OPTSIM. It was altered from 100 lbs to 0 lbs and to 200 lbs. The measured transfer functions are shown in Figure 4. Again, it can be observed that the coherence function is high for the same valid interval of 5-100 Hz. The fundamental modal frequency decreases with increasing bus mass. It can also be observed that the second and third modes are fundamentally different in the case of zero bus mass versus non-zero bus mass. The pole/zero sequence changes, as well as the modal frequencies. The second and third mode in the zero mass case increase by a large amount (to about 34 Hz and 60 Hz).

The concentrated mass entry was changed in the updated NASTRAN model, and the resulting transfer functions can be seen in Figure 4(b). The features that were present in the experimental transfer function

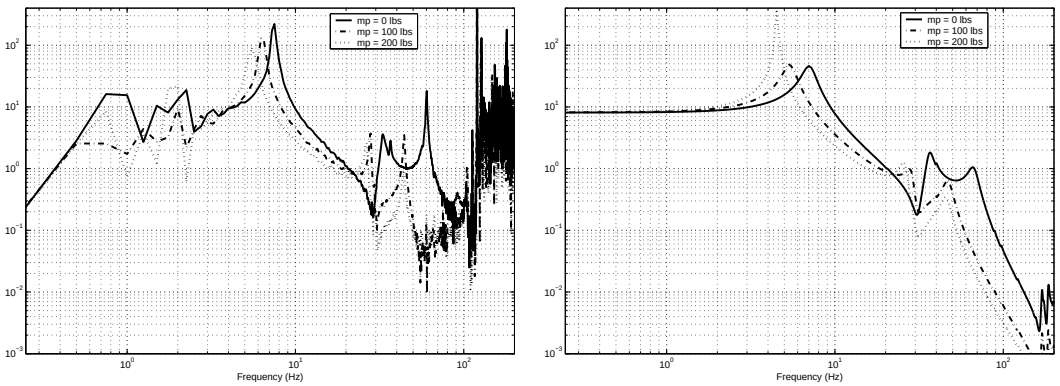

Figure 4. (a) Experimental Transfer Functions $\frac{\mu m}{N}$ for Varying Bus Mass (b) Simulation Model Transfer Functions $\frac{\mu m}{N}$ for Varying Bus Mass

Table 5. Model and Experimental Modes for Three Configurations

Configuration: $m_p = 0$ lbs		
Mode No.	Experimental Modes	Model Modes
First	7.50	7.07
Second	33.00	36.37
Third	60.25	66.97
Configuration: $m_p = 100$ lbs		
Mode No.	Experimental Modes	Model Modes
First	6.25	5.48
Second	28.00	30.02
Third	44.25	49.73
Configuration: $m_p = 200$ lbs		
Mode No.	Experimental Modes	Model Modes
First	5.50	5.26
Second	26.50	25.94
Third	43.75	45.83

look to be repeated fairly well in the simulation model. While the new pole/zero sequence for the $m_p = 0$ lbs configuration tracks well, the modal damping ratios for all three modes seem to be too large in the model. Also the second and third modes are slightly over-predicted. The model for the $m_p = 200$ lbs configuration, tracks extremely well to the experimental, in terms of modal frequency for the second and third mode. The frequency for the first mode, however, is increased. One could conclude then, that the presence of bus mass presents a uniquely different problem, most likely due to the behavior of the base plate under loading. Table 5 shows the modal frequencies in the three configurations.

The objective cost function for the 0 lbs, 100 lbs, and 200 lbs configurations using the tuned model are $J_1 = 1.6968$, $J_t = 1.3942$, and $J_2 = 3.3091$, respectively. The 200 lbs configuration seems to deviate significantly from the original configuration. Applying Equations 5 and 6, to OPTSIM gives,

$$\frac{\|\mathbf{Y}\|_\infty}{(k+1)} = 3.63 \tag{7}$$

The multi-configuration metric is extremely large, exceeding by a wide margin the maximum value recommended

Table 6. Comparison of Updated Parameter Values

Parameters	Original Value	Updated Value	Percent Change
Spring Constant	29198.27	3.0658e+4	5.0
Young's Modulus (Plate)	7.20+10	6.4800e+10	-10.0
Young's Modulus (Links)	7.20+10	7.7767e+10	8.0
Damping ratio 1^{st}	0.01	0.0876	876.0
Damping ratio 2^{nd}	0.01	0.0487	487.0
Damping ratio 3^{rd}	0.01	0.0672	672.0

Parameters	Manually Updated Values	Percent Change
Spring Constant	3.7e+4	+23.3
Young's Modulus 1st Material Card	6.00+10	-16.7
Damping ratio 1^{st}	0.01	0.0
Damping ratio 2^{nd}	0.01	0.0
Damping ratio 3^{rd}	0.01	0.0

Table 7. Table of Objective Function Costs and Multi-Configuration Metrics

Configuration	After Step 1	Updated Model	Man. Updated Model
$m_p = 0$ lbs	-	1.70	2.80
$m_p = 100$ lbs	4.43	1.39	1.07
$m_p = 200$ lbs	-	3.31	1.47
$\frac{\|\mathbf{Y}\|_\infty}{(k+1)}$	-	3.63	4.32

in section 4.3 (2.0). This value could be improved by modifying or augmenting the set of tuning parameters. This value could also indicates that there is still some non-parametric error in the model, so the modeling assumptions should be re-examined.

5.5. Comparison to Manually Tuned Model

The initial model, the experimental data (all three configurations), and the DOCS plotting tools were presented to a colleague, who then tuned the model in the best way he saw fit. He investigated the model for changeable parameters, examined the testbed for possible sources of parametric variation, examined the data supplied for the material cards, and then used trial and error to adjust the Young's modulus of the material cards and the spring stiffness. He assumed that there was no non-parametric error present in the model, but he also noted that non-parametric error could still be a large contributor to model error. The result of the tuning was to increase (from the initial model) the Young's modulus of the first material card 23.3% from 30 kN/m to 37 kN/m and to decrease the spring stiffness from 72 GPa to 60 GPa, a change of -16.7%. The first material card corresponds to the aluminum used for the small and large truss beams, the central bar, the top plate and the outer sandwich plates. Table 6 shows these changes and compares them with the previously tuned model. The first material card corresponds to the aluminum used for the small and large truss beams, the central bar, the top plate and the outer sandwich plates. He also noted that he had severe reservations about the appropriateness of the changed parameters, especially since the new Young's modulus appeared to be non-physical when consulting material tables for aluminum. The experimental and manually tuned model transfer functions seem extremely well matched for this configuration (shown in Howell[8] on page 131). The associated objective function cost is 1.0745, even lower than the cost associated with the tuned model at the end of Step 2. When the configuration is changed, however, the costs go to 2.8001 and 1.4736 for 0 lbs and 200 lbs, respectively. Table 7 shows the cost for the model tuned with the three step procedure versus the manually tuned model. The multi-configuration

metric is

$$\frac{\| \mathbf{Y}\|_\infty}{(k+1)} = 4.32. \tag{8}$$

The manually tuned model had a higher multi-configuration metric than the model tuned using the three step procedure due to the cost of the 0 lbs configuration. Recall that the pole/zero sequence in the transfer function changed in the zero bus mass case. The model tuned using the three step procedure tracks this configuration change better than the manually tuned model, which supports the hypothesis laid out in Section 1. Furthermore, if a model tracks well across configurations, then it also indicates that the model is a good representation of the physical system.

6. SUMMARY AND CONCLUSIONS

This work presented a step-by-step process for model updating of large complex opto-mechanical systems. The focus was on open-loop structural systems, but by integrating the model into one state-space system, these methods can be applied to multi-disciplinary systems. The first step was to apply engineering insight to an initial simulation model. This consisted of several different types of model heuristics intended to create a model in which all the physical systems were represented. The second step, automated tuning, consists of parameter selection, objective function selection, and optimization problem setup. The third step provides a new metric which evaluated how well the tuned model from Step 2 tracked across configurations. This three step process was applied to a complex structural testbed at MIT, and the results were presented. The hypothesis that the three step procedure will produce a model that more effectively tracks along configuration changes was supported by experimental data. Specifically, the multi-configuration metric, which measures how well a particular model tracks the experimental model across configurations, was found to be better in the model that was tuned using the three-step method as opposed to a model using traditional methods (trial and error parameter changing).

These cost values are evaluated as described in Section 4.3. If this evaluation is found to be deficient, it can be assumed that the parameters were not changed properly in Step 2 for the original configuration. Consequently, Step 2 needs to be repeated with an altered formulation. One way to alter the algorithm presented in Step 2 is to narrow the bounds on the chosen parameters. Another way is to change the number of parameters by including some that were initially discarded. Ultimately the formulation in Step 2 is dependent upon the modeler's understanding of the system. It is assumed that Step 1 was implemented properly, since Step 1 consisted of applying engineering insight and systematic error checking. However, further non-parametric error checking might be required in order to produce a physically appropriate system.

After applying Step 1 to OPTSIM, it was found that in order to match the experimental data well, the parameters (spring constant and Young's modulus of the top aluminum plate and rotational links) need to be altered well beyond their bounds. Future work would include a detailed procedure for going back to Steps 1 and 2 and changing the model tuning. Another aspect which should be addressed is the tracking of the modeshapes (eigenvectors) throughout the optimization process in order to make sure that the experimental and model modes are matched properly. Also, this procedure should be applied to a truly multi-disciplinary system, such as one that includes optics and controls. This will require careful incorporation, because controlled systems usually either design a controller that can address a wide variety of disturbances, or make use of on-orbit system identification. In order to build such a controller, an accurate model of the system is needed. If optics were added before the controls, then steps should be taken to ensure the model's accuracy. A useful validation of this work would be to add more inputs and outputs, and apply the three step procedure to a MIMO system. One could also investigate combining Steps 2 and 3, and perform multi-configuration tuning at the same time, in the presence of all the experimental data from all the configurations. This would reduce the iteration effort between Step 2 and Step 3 procedures. Subsystem assembly and the interfaces between subsystems is an important topic for multidisciplinary systems and should be addressed in the future.

ACKNOWLEDGMENTS

This work was supported by the National Defense Science and Engineering Graduate Fellowship program. The manually tuned model of OPTSIM was provided by Scott Uebelhart, a doctoral student in the MIT Space Systems Laboratory.

REFERENCES

1. J. Melody and G. W. Neat, "Integrated Modeling Metholdology Validation Using the Micro-prescision Interferometer Testbed: Assessment of Closed-loop Performance Prediction Capability," in *Proceedings of the American Control Conference*, American Control Conference, June 1997. Albuquerque, NM.
2. H. L. Gutierrez, *Performance Assessment and Enhancement of Precision Controlled Structures During Conceptual Design*. PhD thesis, Massachusetts Institute of Technology, Department of Aeronautics and Astronautics, 1999.
3. O. L. de Weck, "Integrated Modeling and Dynamics Simulation for the Next Generation Space Telescope," Master's thesis, Massachusetts Institute of Technology, June 1999.
4. S. Shaklan, J. Yu., and H. Briggs, "Integrated Structural and Optical Modeling of the Orbiting Stellar Interferometer," **1945**, pp. 123–132, SPIE Conference on Space Astronomical Telescopes and Instruments II., April 1993.
5. R. M. Glaese and D. Miller, "Development of Zero-Gravity Structural Control Models from Analysis and Ground Experimentation," Master's thesis, Massachusetts Institute of Technology, January 1994.
6. M. E. Campbell and E. Crawley, *Uncertainty Modeling for Structural Control Analysis and Synthesis*. PhD thesis, Massachusetts Institute of Technology, January 1996.
7. A. E. Stockwell, "A Verification Procedure for MSC/NASTRAN Finite Element models," NASA Contractor Report 4675, NASA Langley Research Center, May 1995.
8. D. Howell, "Multi-Configuration Model Tuning for Precision Opto-Mechanical Systems," Master's thesis, Massachusetts Institute of Technology, http://ssl.mit.edu/publications/theses/SM-2004-HowellDeborah.html, Februrary 2004.
9. D. J. Ewins, *Modal Testing: Theory, Practice, and Application*, Research Studies Press Ltd., second ed., 2000.
10. N. Maia, *Theoretical and Experimental Modal Analysis*, John Wiley and Sons, 1997.
11. W. Gawronski, *Dynamics and Control of Structures, A Modal Approach*, Mechanical Engineering Series, Springer-Verlag, 1998.
12. E. F. Crawley and S. Hall, "Course notes: Dynamics of controlled structures," 1991.
13. J. Lipkins and U. Vandeurzen, "The Use of Smoothing Techniques for Structural Modification Applications," in *Proceedings of the 12th International Seminar on Modal Analysis*, 1987.
14. R. Harder and R. Desmarais, "Interpolation Using Surface Splines," *Journal of Aircraft* **9**, pp. 189–191, 1972.
15. R. Allemang and D. Brown, "A Correlation Coefficient for Modal Vector Analysis," *Proceedings of the 1st International Modal Analysis Conference* , pp. 110–116, 1982.
16. H. Natke, "Updating Computational Models in the Frequency Domain Based on Measured Data: A Survey," *Probabilistic Engineering Mechanics* **3**(1), pp. 28–35, 1988.
17. C. C. Flanigan, "Test/Analysis Correlation Using Design Sensitivity and Optimization," SAE, 1987. Paper 871743.
18. B. Caesar, "Updating System Matrices Using Model Test Data," International Modal Analysis Conference (IMAC), 1987.
19. N. Maia, M. Reynier, and P. Ladeveze, "Error Localization for Updating Finite Element Models Using Frequency Response Functions," *International Modal Analysis Conference* , pp. 1299–1308, 1994.
20. C. Blaurock, *DOCS User's Guide*. MIDE Technology Corporation, Medford, MA, 2003.
21. O. d. W. Miller, D.W. and G. Mosier, "Framework for Multidiscipliary Integrated Modeling and Analysis of Space Telescopes," in *First International Workshop on Integrated Modeling of Space Telescopes*, *First International Workshop on Integrated Modeling of Telescopes* , SPIE/ESO, February 2002.
22. G. N. Vanderplaats, *Numerical Optimization Techniques for Engineering Design*, Vanderplaats Research and Development Inc, 3rd ed., 2001.
23. P. Y. Papalambros and D. J. Wilde, *Principles of Optimal Design - Modeling and Computation*, Cambridge University Press, 2nd ed., 2000.
24. O. L. de Weck, *Mulitvariable Isoperformance Methodology for Precision Opto-Mechanical Systems*. PhD thesis, Massachusetts Institute of Technology, August 2001.
25. F. Beer and E. R. J. Jr., *Mechanics of Materials*, McGraw-Hill, Inc., 2nd ed., 1992.